

Gel Dehydration by Spontaneous Imbibition of Brine From Aged Polymer Gel

B. Brattekkås, Å. Haugen, A. Graue, SPE, University of Bergen; and
R.S. Seright, SPE, Petroleum Recovery Research Center of New Mexico Tech

Summary

This work investigates dehydration of polymer gel by capillary imbibition of water bound in gel into a strongly water-wet matrix. Polymer gel is a crosslinked-polymer solution of high water content, where water can leave the gel and propagate through porous media, whereas the large 3D polymer-gel structures cannot. In fractured reservoirs, polymer gel can be used for conformance control by reducing fracture conductivity. Dehydration of polymer gel by spontaneous imbibition (SI) contributes to shrinkage of the gel, which may open parts of the initially gel-filled fracture to flow and significantly reduce the pressure resistance of the gel treatment. SI of water bound in aged Cr(III)-acetate-hydrolyzed-polyacrylamide (HPAM) gel was observed and quantified. Oil-saturated chalk-core plugs were submerged in gel, and the rate of SI was measured. Two boundary conditions were tested: all faces open (AFO) and two-end-open oil-water (TEO-OW), where one end was in contact with the imbibing fluid (gel or brine) and the other was in contact with oil. The rate of SI was significantly slower in gel compared with brine, and was highly sensitive to the ratio of matrix volume to surface open to flow, decreasing with increasing ratios. The presence of a dehydrated gel layer on the core surface lowered the rate of imbibition; continuous loss of water to the core increased the gel layer concentration and thus the barrier to flow between the core and fresh gel. Severe gel dehydration and shrinkage up to 99% were observed in the experiments, suggesting that gel treatments may lose efficiency over time in field applications where a potential for SI exists. The implications of gel dehydration by SI, and its relevance in field applications, are discussed for both gel and gelant field treatments.

Introduction

Oil recovery from fractured reservoirs poses great challenges to the exploration-and-production industry. Fractures often exhibit permeabilities several orders of magnitude higher than the rock matrix, which may cause injected fluids to channel through fracture networks rather than displacing oil from the matrix. This can lead to early water breakthrough and low sweep efficiency. By reducing fracture conductivity, sweep efficiency and oil recovery may be significantly improved (Graue et al. 2002). Injection of polymer gels to reduce flow in high-permeability zones or fractures has been reported (Portwood 1999, 2005; Seright 2003; Rousseau et al. 2005; Syndansk and Southwell 2000; Willhite and Pancake 2004). Reducing fracture conductivity by use of gels may increase the differential pressure across matrix blocks during subsequent waterfloods or chemical floods, and injected fluids can be diverted into regions that have not previously been swept. Two approaches have been studied: injection of immature gel (gelant) and injection of preformed gel. Gelant treatments are favorable for matrix treatments because low viscosity and small particles allow the solution to flow through the matrix (Seright et al. 2003). A polymer gel is often formed by subjecting a lower-viscosity gelant to a higher temperature over a certain time period, during

which the solution changes into a highly viscous and rigid gel. Injection of preformed polymer gel may reduce injectivity, but has been shown to have little sensitivity to physiochemical conditions in a reservoir and ensures treatment of the fractures only, because the formed gel does not penetrate significantly into porous rock (Seright 2001; Zhang and Bai 2011). Thus, productive oil zones will not be harmed and the chemical treatment is limited to the small fraction of the reservoir formation that constitutes the fracture volume [approximately 1% pore volume (PV)]. Polymer gels have an initial water content of 95 to 99.7% (Syndansk 1993), which may be reduced by a leakoff process that can occur when preformed gel propagates through fractures (Seright 2001, 2003). During leakoff, water escapes the gel and may progress through the fracture surfaces, leaving gel in the fracture more concentrated and rigid. The pressure resistance of the gel, and thus its ability to divert chase water, increases with increasing polymer concentration. A model for leakoff was proposed by Seright (2003), and was shown to be valid for Portland chalk during traditional leakoff experiments when the injection rate was held constant (Brattekkås 2009).

After placement, the gel may undergo processes that jeopardize its resistance to pressure. These are, for example, syneresis (Vossoughi 2000; Romero-Zeron et al. 2003) and dehydration. Dehydration is characterized by a reduction of the gel volume caused by the expulsion of solvent from the gel, and has previously been observed during fluid flow through micromodels containing gel (Dawe and Zhang 1994; Al-Sharji et al. 1999) and through bulk volumes of gel (Krishnan et al. 2000). These authors suggested that imposing a pressure gradient on a bulk volume of gel after placement may dehydrate the gel. Dehydration was caused by an imbalance of forces on either side of the gel/fluid interface, and was dependent on the rigidity of the gel.

Although gel behavior after placement in fractures has been widely studied, results are rarely discussed in conjunction with the properties of an adjacent, oil-saturated, porous medium. The effect that relative permeability and capillary pressure in the porous matrix may have on gel behavior in fractured reservoirs is even less discussed. This work verified experimentally that an exchange of fluids between the gel and adjacent matrices may occur by spontaneous capillary imbibition of water from the gel, without imposing a pressure gradient on the system. The occurrence of SI indicated that gel behavior during and after placement may be dependent on matrix properties, above all wettability. The wettability of the matrix dictates the shapes of the relative permeability and capillary pressure curves, which in turn strongly influence fluid flow, and should thus be considered when planning a gel treatment and predicting its efficiency. In a strongly water-wet matrix, a positive capillary force to attract water exists. In an oil-wet matrix, water will be repelled and must overcome a capillary threshold pressure to invade the pores. Other matrix parameters, such as pore-size distribution (rock type) and saturation, will also influence the ease at which the water leaves the gel or fracture and goes on to flood the matrix.

Experiments were performed to investigate whether the capillary forces in outcrop core plugs were strong enough to extract water from formed polymer gel, and to determine the rate and endpoint of SI in chalk. Measuring the rate of SI was important because it suggests whether the SI process in a gel/oil system is different from that in a conventional water/oil system. The gel used in the experiments was a commercially available Cr(III)-

Copyright © 2014 Society of Petroleum Engineers

This paper (SPE 153118) was accepted for presentation at the SPE Improved Oil Recovery Symposium, Tulsa, 14–18 April 2012, and revised for publication. Original manuscript received for review 26 February 2013. Revised manuscript received for review 25 June 2013. Paper peer approved 26 July 2013.

TABLE 1—CORE OVERVIEW				
Core Name	Comment	Experiment Type	Boundary Condition	Saturated With
<u>Spontaneous Imbibition (SI)</u>				
1_SI test	P. chalk	SI in gel	AFO	Decane
2_SI test	B. sandstone	SI in gel	AFO	Decane
3_SI test	E. limestone	SI in gel	AFO	Decane
1_SI		SI in brine	AFO	Lamp oil
2_SI		SI in brine	AFO	Lamp oil
3_SI		SI in gel	AFO	Lamp oil
4_SI		SI in gel	AFO	Lamp oil
5_SI		SI in gel	AFO	Lamp oil
6_SI		SI in gel	AFO	Lamp oil
7_SI		SI in gel	AFO	Lamp oil
1_CC		SI in brine	TEO-OW	Lamp oil
2_CC		SI in brine	TEO-OW	Lamp oil
3_CC		SI in brine	TEO-OW	Lamp oil
4_CC		SI in (1) gel and (2) brine	TEO-OW	Lamp oil
5_CC		SI in (1) gel and (2) brine	TEO-OW	Lamp oil
6_CC		SI in gel	TEO-OW	Lamp oil
7_CC		SI in gel	TEO-OW	Lamp oil
8_CC		SI in gel	TEO-OW	Lamp oil
<u>Gel Shrinkage (GS)</u>				
1_GS		Gel shrinkage	TEO (vertical)	Decane
2_GS	*	Gel shrinkage	TEO (vertical)	Decane
3_GS	**	Gel shrinkage	TEO (vertical)	Decane
4_GS	**	Gel shrinkage	TEO (vertical)	Decane
5_GS		Gel shrinkage	TEO (vertical)	Decane
6_GS		Gel shrinkage	TEO (vertical)	Decane
* Imbibition stopped after first batch of gel, before the endpoint.				
** Several batches of gel added for imbibition.				
Note: CC = cocurrent imbibition.				

polyacrylamide. One of the differences when imbibition occurred in gel compared with brine was the immobile gel layer that formed on the rock surface as a result of gel dehydration. A thickening gel cake was observed as gel dehydrated on the core surface during imbibition, which led to an increasing skin factor that slowed the imbibition process down compared with imbibition in brine.

Experiments were also performed to determine the degree of gel shrinkage caused by imbibition. A high degree of dehydration, and thus shrinkage, was found. This could, in time, open large parts of the gel-treated fractures to flow and decrease the efficiency of the gel treatment. According to numerous authors, gel treatments have in many field applications been less effective than expected in reducing water production from fractured wells, or the treatments have lost efficiency over time (White et al. 1973;

Seright 2003; Portwood 2005). This study may contribute to new understanding of gel failure after treatment in water-wet fields.

Experiments

The experimental schedule was two-fold. First, a set of experiments was conducted to investigate SI rates from cores fully submerged in gel. Two boundary conditions for SI were tested: AFO (all faces open) and TEO-OW (two-end-open oil-water). Core plugs and corresponding boundary conditions are listed in **Table 1**. Next, a set of experiments was conducted to quantify shrinkage of gel driven by capillary SI.

Different experimental setups were required, and there are outlined in the following paragraphs and illustrated in **Fig. 1**.

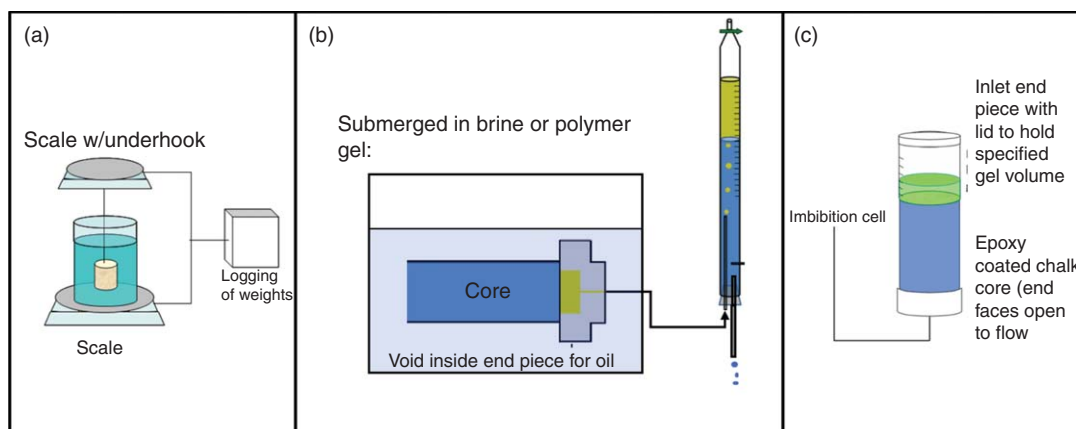


Fig. 1—(a) Schematic of setup for continuous measurements of gel and core weight vs. time using AFO boundary conditions. (b) Schematic of setup for cocurrent imbibition with TEO-OW boundary conditions. (c) Schematic of setup for gel-shrinkage experiments.

TABLE 2—CORE PROPERTIES

Core Name	Length (cm)	Diameter (cm)	Area Open for Imbibition (cm ²)	Volume/Open-Surface Ratio (cm)	Pore Volume (mL)	Porosity (%)	S _o Endpoint to Gel (%)	S _o Endpoint to Water (%)
<u>Spontaneous Imbibition (SI)</u>								
1 SI test	9.1	3.80	131.32	0.79	45.53	44.12	68.3	68.3
2 SI test	5.92	3.80	93.36	0.72	14.27	21.26	66.97	66.97
3 SI test	8.84	3.80	128.21	0.78	16.6	16.56	52.84	52.84
1_SI	6.04	5.09	137.28	0.90	53.76	43.74	—	62.13
2_SI	6.04	5.07	136.58	0.89	54.05	44.33	—	62.53
3_SI	7.97	5.09	168.04	0.96	75.11	46.36	65.11	65.11
4_SI	7.92	5.09	167.26	0.96	75.92	47.14	59.48	59.48
5_SI	7.92	5.07	166.59	0.96	77.81	48.63	57.41	57.41
6_SI	8.01	5.10	169.19	0.97	77.28	47.23	56.34	56.34
7_SI	8.02	5.07	167.91	0.96	75.92	46.98	60.54	60.54
1_CC	6.00	3.79	11.28	6.00	33.42	49.37	—	61.64
2_CC	6.00	3.82	11.46	6.00	33.14	48.19	—	57.64
3_CC	10.51	3.79	11.28	10.51	56.03	47.25	—	57.12
4_CC	6.00	3.80	11.34	6.00	33.67	49.48	44.03	54.3
5_CC	10.30	3.80	11.34	10.30	56.57	48.17	47.18	52.27
6_CC	6.00	3.80	11.34	6.00	27.34	40.17	43.16	43.16
7_CC	10.30	3.80	11.34	10.30	47.06	40.28	24.01	24.01
8_CC	10.45	3.80	11.34	10.45	51.76	43.67	22.21	22.21
<u>Gel Shrinkage (GS)</u>								
1_GS	5.23	3.72	10.87	5.23	26.71	46.99	64.69	—
2_GS	6.89	3.74	10.96	6.89	34.88	46.20	28.32	—
3_GS	12.62	3.65	10.43	12.62	56.21	42.68	53.04	63.00
4_GS	11.85	3.61	10.24	11.85	52.96	43.66	60.76	64.91
5_GS	6.01	3.88	11.82	6.01	32.23	45.36	56.57	56.57
6_GS	6.03	3.84	11.58	6.03	31.54	44.24	58.97	59.76

Core Material and Preparation. Chalk blocks were obtained from the Portland Cement Factory in Aalborg, Denmark, and cylindrical core samples of various diameters and lengths were drilled out. The rock formation is Maastrichtian and consists mainly of coccolith deposits. The composition is to a large extent calcite (99%) with some quartz (1%). The brine permeability and porosity ranges from 1 to 10 md and 43 to 48%, respectively. More details about the rock may be found in Ekdale and Bromley (1993) and Hjuler (2007). Edwards limestone from a quarry in west Texas, USA, was used in an introductory experiment. Trimodal pore sizes, vugs, and microporosity have been identified by use of thin-section images, mercury injection, and nuclear-magnetic-resonance T_2 relaxation experiments, respectively. The brine permeability and porosity range from 3 to 28 md and 16 to 24%, respectively (Riskedal 2008; Tipura 2008). Bentheim sandstone from the Gildehausen quarry near Bentheim, Germany, was also used. The Bentheim sandstone is homogeneous in terms of porosity and permeability, averaging at 23% and 1,100 md, respectively, with mean composition of 95% quartz, 3% kaolinite, and 2% orthoclase. More information may be found in Klein and Reuschlè (2003) and Schutjens et al. (1995).

Twenty-four core plugs were prepared for this study. All cores were washed and dried at 80°C for several days before they were vacuum evacuated and saturated directly with oil. When comparing imbibition processes in several core samples, we desire similar initial fluid distributions. In this work, this was fulfilled by saturating all cores initially 100% with oil. Previous experiments on this core material and wettability showed that the rate of imbibition increased with S_{wi} up to approximately 34% and then decreased with further increase in S_{wi} (Viksund et al. 1998), which means that the SI of solvent from gel would be even quicker with irreducible water saturation present, provided that this is less than 34%. The porosity and PV of each core plug were determined from weight measurements. Cores used for TEO-OW boundary-condition experiments and gel-shrinkage experiments were coated

with epoxy along the core length so only the end faces were open to flow. A polyoxymethylene (POM) end piece was fitted at one end of the TEO-OW cores, through which oil was produced and directly quantified during imbibition. Cores used in gel-shrinkage experiments were fitted with a POM end piece at the outlet end and a plastic container at the inlet, to hold a specified gel volume. After saturation, the cores were subjected to SI tests in brine or preformed polymer gel. All experiments were performed at ambient temperature. An overview of all cores and experiments is shown in Table 1, and core properties may be found in **Table 2**.

Fluids. The gel used was 0.5% HPAM (Ciba Alcoflood 935, approximately 5 million daltons molecular weight) crosslinked by 0.0417 wt% (417 ppm) Cr(III)-acetate and aged at 41°C for 24 hours (five times the gelation time). After aging, the gel was cooled to ambient temperature and imbibition experiments started. Sydansk gel codes were C to D. The fluid properties of all fluids used are given in **Table 3**.

Spontaneous Imbibition (SI). Initial experiments were performed by use of three outcrop core materials of different capillarity: 1 SI test, 2 SI test, and 3 SI test (Tables 1 and 2). The cores were saturated with oil and dropped in beakers containing aged gel. The induction time was recorded, and the cores were left in the beakers until SI ended. At this point, the cores were weighed and recovery was calculated from material balance equations. The rates of oil recovery and SI were not measured for these cores, and the endpoints were estimated from visual observations. For Cores 1_SI through 7_SI and 1_CC through 8_CC, imbibition rates were determined during SI with cores fully submerged in either brine or gel by use of one of two boundary conditions.

The AFO boundary conditions included the following steps: The rate of SI vs. time was quantified by gravimetric measurements of the core sample and brine or gel, respectively, by use of

TABLE 3—FLUID PROPERTIES			
Fluid	Density (g/cm ³)	Viscosity (10 ⁻³ Pa·s) at 20°C	Composition
Ekofisk brine	1.048	1.09	4.00 wt% NaCl, 3.40 wt% CaCl ₂ , 0.50 wt% MgCl ₂ , 0.05 wt% NaN ₃
<i>n</i> -Decane	0.73	0.92	—
Refined lamp oil	0.74	1.43	—
HPAM Gel (24 hours old)	≈1.048	≈2×10 ⁶ after gelation*	0.5% HPAM 0.0417% Cr(III)-Acetate Ekofisk brine

* Measured at 0.001-sec⁻¹ shear rate after 24 hours of gelation (Liu and Seright 2001).

the setup showed in Fig. 1a. The core and fluid weights were both logged vs. time. At given timesteps, the core was lifted out of the brine or gel bath by the strings attached to the weight, excess fluid (oil drops and nondehydrated gel) was carefully wiped off the surface, and the core was weighed. This approach was used because a steadily increasing gel film occurred on the core surface during SI in gel, which captured the displaced oil. After weighing, the core was submerged again in the fluid. The displaced oil volume, and hence the rate of recovery, was calculated at each timestep by use of material-balance equations. The core endpoint saturation was determined from weight measurements after imbibition ended. The gel layer on the core surface was also collected and weighed. A thin layer of oil on top of the polymer gel or brine prevented evaporation of water during long-term tests.

TEO-OW boundary conditions were also used. The experimental setup, shown in Fig. 1b, ensured that one end face of the core was in contact with the aqueous imbibing phase and the other with the oleic phase. Zero capillary pressure is obtained at the second end face. Because of capillary pressure being present only at the inlet end face, displacement of oil mainly occurs at the outlet end of the core when the core is aligned horizontally, except for a moment right after imbibition begins. This makes it possible to quantify the bulk of the oil production directly by volume recordings, also during imbibition in gel. After imbibition in gel ceased, the dehydrated gel layer was removed from the inlet end face and all cores were submerged in brine for further SI.

Gel Shrinkage. One of the most important applications of SI of water from gel is gel shrinkage; blocking of fractures by gel is most efficient if the entire fracture volume, or significant parts of it, is filled with low-permeability gel. Gel shrinkage is here defined as the percentage of initial gel volume that is lost because of spontaneous capillary imbibition of water from the gel. Shrinkage of gel during SI was measured by exposing an oil-saturated core plug to a limited volume of gel and recording the reduction in gel volume during SI. The setup was similar to TEO-OW, but the cores were placed vertically with a specified gel volume on top. This ensured contact between the gel and rock surface at all times. The shrinkage of gel by SI was recorded directly by volume measurements. At the endpoint, the gel film was collected and weighed to determine total gel shrinkage. If the endpoint for SI was not reached by use of one batch of gel, one or several more batches of gel could be added to the plastic container. After removal of the final gel layer, brine was placed in the container to ensure that the potential endpoint for imbibition was reached, or to define the final endpoint. A schematic of the setup is showed in Fig. 1c.

Results and Applications

SI. SI of water from preformed gel was first observed in three cores—1 SI test (chalk), 2 SI test (sandstone), and 3 SI test (limestone)—that were fully saturated with oil and placed in beakers of aged polymer gel. The SI process dehydrated gel close to the core surface and continued until the endpoint for imbibition was

reached in the cores, regardless of capillarity. The induction time was, however, influenced by capillarity and was shortest in chalk (1.5 minutes) compared with Edwards limestone (11 minutes) and Bentheim sandstone (53 minutes). The rate of imbibition was not measured in the first three experiments, but the procedure was extended in the next 15 core plugs—1_SI through 7_SI by use of AFO boundary conditions and 1_CC through 8_CC by use of TEO-OW boundary conditions—to make these measurements possible. Visual recordings were challenging for AFO cores, because displaced oil volumes were trapped in the gel and could not be separated from it and accurately measured, either during SI or after the process ended. Weight measurements were therefore used for monitoring the development in average oil and water saturations during imbibition. During SI, gel dehydrates on the core surface and forms a filter cake of more-concentrated gel. This filter cake influences the accuracy of the gravimetric measurements; the layer of dehydrated gel will add to the core weight and overestimate the recovery if it is not accounted for. Intuitively, the amount of dehydrated gel on the core surface will depend on the amount of water imbibed. This means that the immobile gel layer will increase faster when the rate of SI is higher. The development of the gel layer vs. time, quantified by the weight of dehydrated gel, will thus mimic the SI curve and may be determined by use of Eq. 1,

$$m_{gf}(t) = \frac{\Delta m(t)}{\Delta m_{\max}} \times m_{gf,\max} = \frac{[m_{(c+gf)}(t) - m_i]}{[m_{(c+gf),\max} - m_i]} \times m_{gf,\max}, \quad \dots \dots \dots (1)$$

where $m_{gf}(t)$ is the gel film weight as a function of time, $\Delta m(t)$ is the difference between the initial weight, m_i , and the weight of the core (including gel film) as a function of time, $m_{(c+gf)}(t)$. Δm_{\max} is the maximum weight change; the difference between initial and endpoint core weights (including the gel film) is $m_{(c+gf),\max}$. $m_{gf,\max}$ is the gel film weight at the endpoint of SI, and is found by weighing the core with and without the gel layer. Eq. 1 is simply a material balance. The removal of the gel layer must be performed cautiously because the material-balance calculations depend on the core being intact throughout the experiment. Fig. 2 shows Core 1_SI Test during imbibition, and illustrates the oil drops that were trapped by gel on the core surface or in the core vicinity.

Fig. 3 shows the recovery of oil during SI for Cores 1_SI through 7_SI, scaled in accordance with Ma et al. (1997). The black lines represent the SI curves for brine, whereas the gray lines show the imbibition curves for cores submerged in gel. The imbibition in gel was a factor 10 slower than imbibition in brine. The endpoint for SI, equal to the residual oil saturation (ROS) for this particular core material (Viksund et al. 1998), was reached in all experiments, including those when the cores were submerged in gel. The endpoint was confirmed by placing the cores in brine for further SI after removal of the dehydrated gel layer. Every marker in Fig. 3 represents a point in time when the cores have been taken out of the brine or gel bath and weighed in air. The cores were extracted from the gel by lowering the gel bath, hence



Fig. 2—Oil adhesion to the core surface during imbibition.

leaving the cores suspended in the strings attached to the weight. The rigid gel (in which the cores were submerged) detached from the cores quite easily, which may be because of weak bonds between the gel film on the core surface and gel in the gel bath.

Excess gel and oil drops were removed from the core surfaces before weighing, but the dehydrated gel film was left unharmed. Fig. 4a shows the imbibition rates in both water and gel, and Fig. 4b shows the imbibition rates in gel only. The imbibition rates were severely reduced when cores were submerged in gel instead of brine, although the induction time was the same: Oil production was observed approximately 90 seconds after core immersion in both gel and brine. Weight recordings started at Core 4_SI, time of 91 minutes; Core 5_SI, time of 10 minutes; and Cores 6_SI and 7_SI, time of 2 minutes after initially submerging the cores in gel. Both oil recovery and the rate of SI were lower at a given time when the first weight recording was made later in the experiment. During SI in gel, Core 4_SI therefore had the lowest rate of recovery, Core 5_SI had a slightly higher rate, and Cores 6_SI and 7_SI had the highest rates of recovery and imbibition. The reason for this behavior may be the filter-cake formation on the core surfaces during imbibition; soon after immersion in aged gel, the dehydrated gel layer is thin and may be partially removed together with the oil drops and excess gel at weighing, which will make the core surface more easily accessible for further SI. This was confirmed by partially removing gel from Core 7_SI at Timesteps

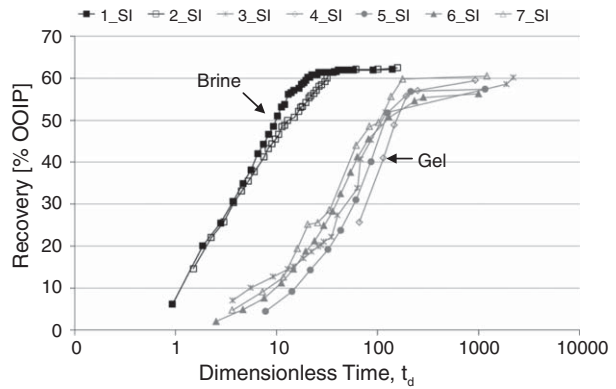


Fig. 3—Oil recovery during SI.

3, 4, 10, and 11, which resulted in a more rapid SI in the core and higher recovery values at the subsequent timesteps. The rate of recovery was comparable with Core 6_SI, when the dehydrated gel layer was left undamaged. Core 3_SI was not weighed in air, but left in the container for the whole duration of the experiment. Consequently, oil-drop adhesion to the core surface was not corrected for, and oil recovery was overestimated early in the experiment. Large-scale disturbances were experienced in the data set because of oil drops growing and letting go of the core surface, thus Core 3_SI was omitted when calculating imbibition rates.

To enable visual recordings, and thus enhance the accuracy of the measurements, cores with TEO-OW boundary conditions were prepared. During SI experiments in brine by use of these boundary conditions, countercurrent production of oil occurred for a short initial period, producing minor amounts of oil (corresponding to 2 to 4% of the total core PV) at the inlet end. The remainder oil volume was produced at the outlet end, hence direct recordings of outlet-end oil production reflected the imbibition process in the core and when the fluid contacting the inlet end face was gel. Oil production at the outlet end could be recorded volumetrically without removing the core from the imbining fluid. Cores 1_CC, 2_CC, and 3_CC were subjected to cocurrent SI tests in brine, whereas Cores 4_CC, 5_CC, 6_CC, 7_CC, and 8_CC of similar dimensions were subjected to gel testing. No change in induction time was observed between water and gel imbibition, and oil was produced soon after immersion. The production curves from cocurrent imbibition by use of TEO-OW boundary conditions are shown in Fig. 5.

Fig. 6a shows the imbibition curves as a function of the square root of time for the shorter cores (6 cm), and Fig. 6b for the longer cores (10 cm). The mass of water imbibed is a linear function of the square root of time in water/oil systems (Handy 1960). Oil recovery as a function of the square root of time was not linear in gel/oil systems. The cocurrent imbibition process was slow in both brine and gel, and the ROS was reached after a long period

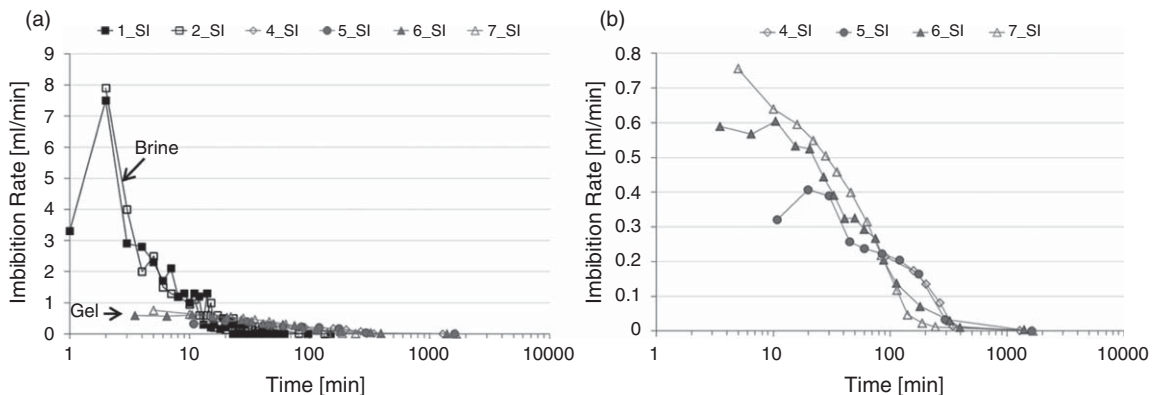


Fig. 4—(a) The rate of SI in brine and gel. (b) The rate of SI in aged polymer gel alone.

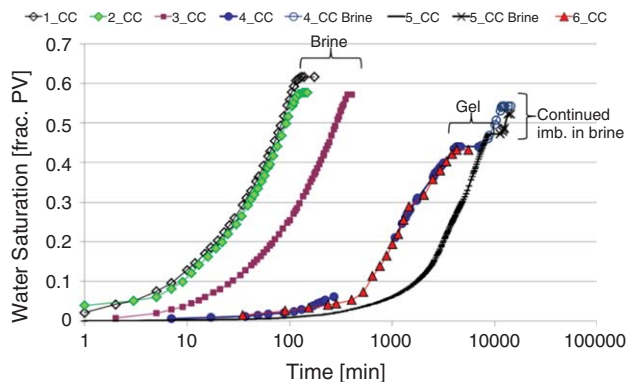


Fig. 5—Recovery during cocurrent imbibition for cores of different lengths (and thus different bulk-volume/open-surface ratios) submerged in brine or gel.

of time when the cores were submerged in brine. During gel testing, the endpoint for SI was not reached, and continued imbibition in brine was possible after gel testing when the filter cake had been removed from the inlet end face. Continued imbibition in brine is denoted in Core 4_CC Brine in Fig. 6a and Core 5_CC Brine in Fig. 6b. For a short time after immersion in brine or gel, countercurrent production of oil was observed. In most cores, countercurrent production was minor and the change to pure cocurrent production was swift. Some cores, however, produced a substantial amount of oil countercurrently. Examples are Cores 7_CC and 8_CC, which produced much of the oil at the inlet end, and imbibition curves could not be generated. Mason et al. (2009) also reported a larger scatter in results when the area that is open to imbibition decreases. Oil produced countercurrently was

trapped in the gel at the inlet and could therefore not be quantified gravimetrically or volumetrically.

A recovery-rate dependency on bulk-volume/open-surface ratio (VSR) was detected during immersion in both brine and gel. The VSR is defined as

$$VSR = V_b/A_{surf}, \dots \dots \dots (2)$$

where V_b is the bulk volume of the core sample (cm^3) and A_{surf} is the surface area open to flow (cm^2). Increasing VSR led to lower recovery rates. The delay caused by increasing VSR values may be corrected by accounting for the dimensional differences: dividing imbibition time by core length squared. The scaled results are shown in Fig. 7. The delay seen between the brine and gel imbibition curves must be caused by interactions between the core surface and the polymer gel, particularly the thickening filter cake on the core surface. Gel particles will not enter the small chalk pores, thus the two-phase flow within each core during imbibition constitutes brine and oil only.

The filter cake that forms on the core surface introduces a skin factor that increases during imbibition as the thickness and concentration of the filter cake grows. The endpoint for SI was not reached during imbibition in gel because capillary forces were counteracted by the skin factor, thus stopping the imbibition process. When imbibition stopped, the dehydrated gel layer that constitutes the filter cake was removed from the end face and the cores were immersed in brine for further imbibition to reach the endpoint.

The rates of imbibition for TEO-OW boundary-condition experiments are shown in Fig. 8. During imbibition in brine, slightly increased initial values were seen, after which the rates slowly decreased. Imbibition ceased at the ROS. Dimensional differences did not influence the imbibition rate, and the longer cores experienced the same rates as the shorter cores, although they

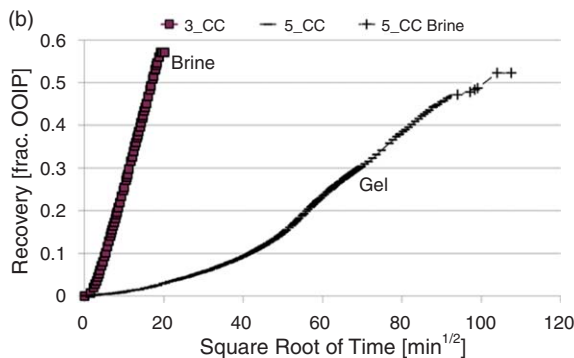
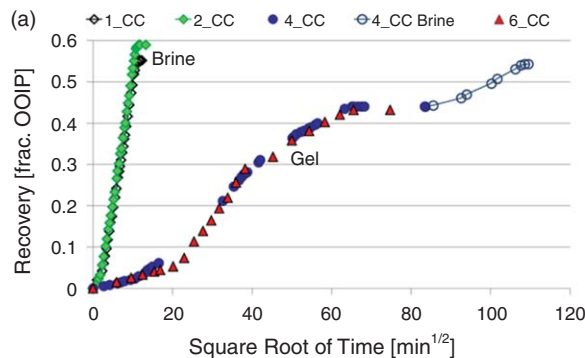


Fig. 6—(a) Recovery vs. the square root of time for 6-cm cores. (b) Recovery vs. the square root of time for 10-cm cores.

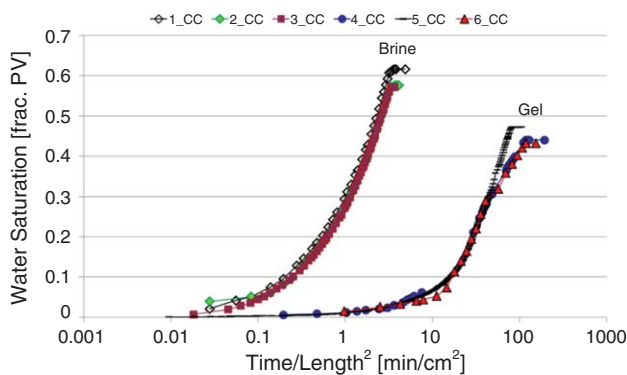


Fig. 7—Recovery during imbibition vs. t/L^2 . The dimensional differences are accounted for by dividing imbibition time by core length squared; thus, the time difference between the curves is because of the polymer-gel characteristics or core-surface/polymer-gel interactions.

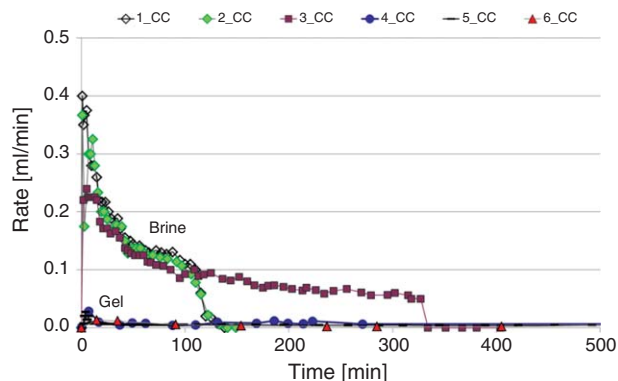


Fig. 8—Rate of cocurrent SI in cores of different lengths and TEO-OW boundary conditions submerged in brine or gel. The x-axis in this case is limited to the time when brine imbibition still occurs.

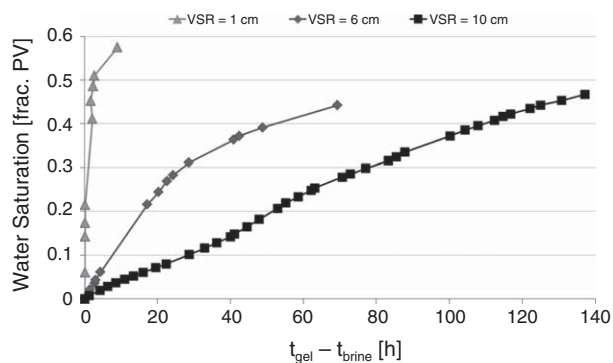


Fig. 9—The additional time it takes to imbibe water during imbibition in gel compared with brine increase with water saturation and increasing VSR.

continued to imbibe water for an extended period of time. During TEO-OW imbibition in gel, the imbibition rates were low, peaking at approximately $0.03 \text{ cm}^3/\text{min}$. At the endpoint, when the filter cake was removed and the cores were placed in brine, the imbibition rates decreased further (approximately $0.001 \text{ cm}^3/\text{min}$). Few visual recordings and slight changes in displaced oil volume per timestep make it difficult to quantify the changes in imbibition rate with tolerable uncertainty. Exact values or graphs will for this reason not be given.

During cocurrent imbibition, the cores submerged in gel required approximately 30 times longer to reach their respective endpoint saturations, which were lower than the recorded endpoints for imbibition in brine. This factor is expected to vary on the basis of the capillarity of the rock, the gel concentration, and the water/oil mobility ratio, and was also shown to vary with VSR. Fig. 9 shows the additional time needed to obtain a given water saturation during imbibition in gel compared with brine for AFO cores (VSR of approximately 1 cm) and TEO-OW cores (different VSRs, of approximately 6 and 10 cm). The curves in Fig. 9 were constructed by subtracting the imbibition time in water from the imbibition time in gel at given water-saturation points for each VSR. Cores with lower VSR achieve high water saturations faster during gel injection than cores of higher ratios. This implies that SI of gel-bound water may be faster and more severe in highly fractured reservoirs, where VSR is lower.

Gel Shrinkage. Six cores were prepared with TEO-OW boundary conditions to measure gel shrinkage, and imbibition experiments were performed with a limited volume of gel available for

imbibition. Shrinkage of gel caused by dehydration during SI was recorded. The available gel volume varied from 0.03 to 1 PV. Table 4 shows data for gel-shrinkage experiments, including available gel volume in milliliters, fraction of PV, and fraction of oil saturation. Initial gel film thickness and volumetric shrinkage after imbibition are also tabulated. Cores 3_GS and 4_GS had four consecutive placements of a known volume of gel, and each placement of gel is tabulated.

Fig. 10 shows shrinkage of the gel film as function of time for each core and gel placement. Because the cores were placed vertically with a gel volume on top, gravitational effects could not be neglected and oil production occurred at the inlet as well as the outlet end, especially at low water saturations. Collection and recording of the oil produced at the inlet end was possible because of the limited amount of gel present, but in many cases a fraction of the oil was bound in the gel and could not be collected until the endpoint for imbibition was reached. All countercurrently produced oil could be collected when the gel film was removed from the core surface, because oil was not dispersed in the gel but merely trapped in it. Some of the curves in Fig. 10 show a sudden increase in gel shrinkage between the two last points because of this; the shrinkage curves of Core 3_GS, the third and fourth gels, and Core 4_GS, the third and fourth gels, exemplify this behavior.

Fig. 11 shows the gel shrinkage curves as functions of the square root of time. Cores with few data points were not included. The core with the highest available gel volume in fraction of PV (Core 6_GS) exhibited the slowest gel shrinkage. After Core 6_GS (available gel volume, $\text{PV} = 0.98$) was Core 1_GS ($\text{PV} = 0.82$) and Core 3_GS, fourth gel placement ($\text{PV} = 0.4$). Core 2_GS ($\text{PV} = 0.30$), Core 4_GS, fourth gel placement ($\text{PV} = 0.29$), and Core 4_GS, second gel placement ($\text{PV} = 0.21$) showed comparable shrinkage trends. Core 4_GS, third gel placement ($\text{PV} = 0.20$), was similar to Core 4_GS, fourth gel placement, up to $t^{1/2} = 30$, but exhibited a higher imbibition rate after this time. Core 3_GS, first gel placement ($\text{PV} = 0.03$), and Core 3_GS, second gel placement ($\text{PV} = 0.1$), had the lowest available volumes of gel and exhibited the fastest gel shrinkage. This behavior is expected; a 10% increase in core water saturation corresponds to a higher degree of gel shrinkage if the available gel volume is low.

Fig. 12a shows the relationship between normalized oil recovery and gel shrinkage: If the available gel volume is less than the potential volume for SI, gel shrinkage is fairly predictable for this rock/oil/gel system. For the two cores where the available gel volumes exceeded the imbibition potential, however, the gel shrinkage decreased. Fig. 12b shows the degree of gel shrinkage plotted against the gel volume available for SI. The curve is a third-degree polynomial fit to the experimental data and shows that the

TABLE 4—GEL-SHRINKAGE-EXPERIMENT SPECIFICS

Core Name	Gel Placement (No.)	Available Gel			Initial Gel Film Thickness (cm)	Shrinkage (%)
		(mL)	(Fraction of PV)	(Fraction of S_o)		
1_GS	1st	21.81	0.82	0.82	2.01	79.22
2_GS	1st	10.28	0.29	0.29	0.94	98.28
3_GS	1st	1.92	0.03	0.03	0.18	98.26
	2nd	5.25	0.09	0.10	0.50	95.27
	3rd	7.96	0.14	0.16	0.76	95.80
	4th	18.13	0.32	0.44	1.74	97.16
	Total	33.25	0.59	—	—	—
4_GS	1st	6.64	0.13	0.13	0.65	98.13
	2nd	9.87	0.19	0.21	0.96	95.26
	3rd	7.59	0.14	0.20	0.74	94.59
	4th	9.65	0.18	0.29	0.94	94.16
	Total	33.74	0.64	—	—	—
5_GS	1st	19.27	0.60	0.60	1.63	94.65
6_GS	1st	30.84	0.98	0.98	2.61	60.31

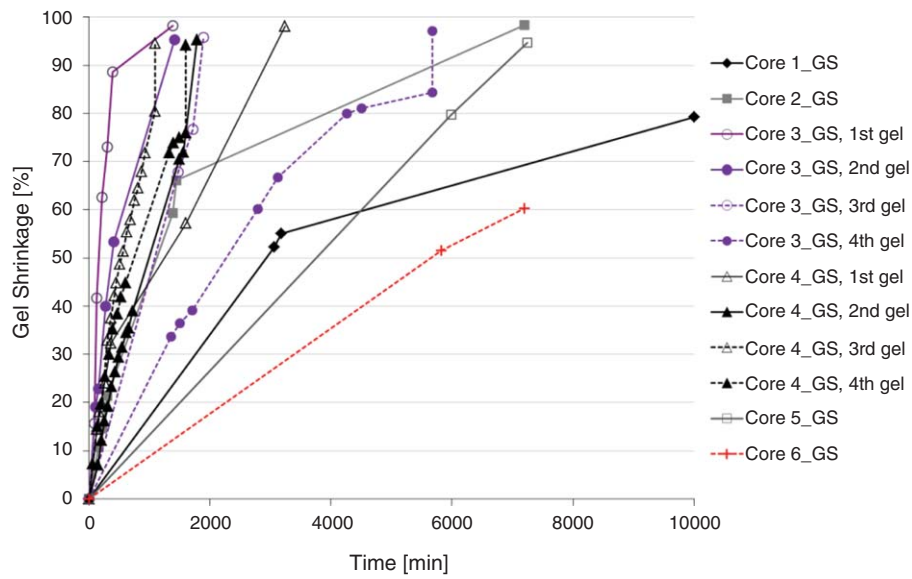


Fig. 10—Gel shrinkage as a function of time for SI cores.

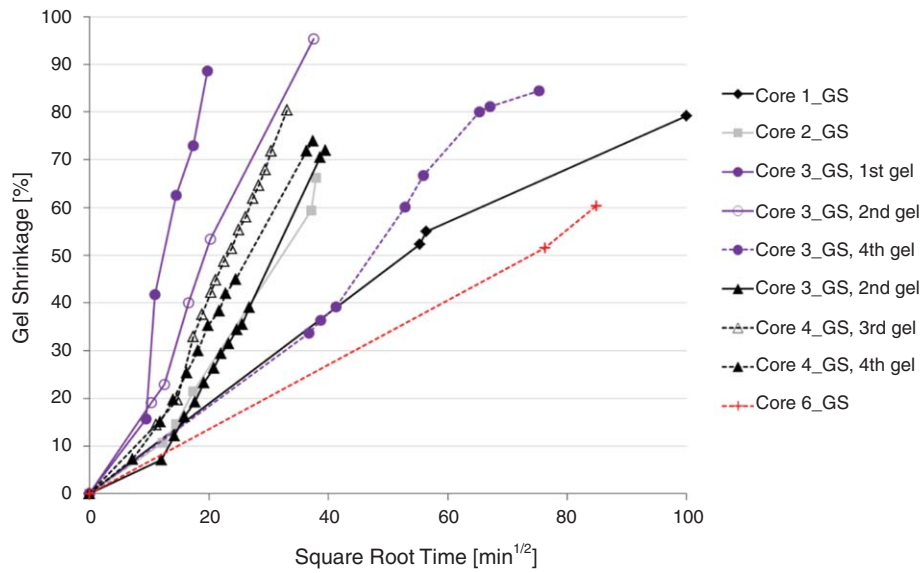


Fig. 11—Gel shrinkage as a function of the square root of time for some cores.

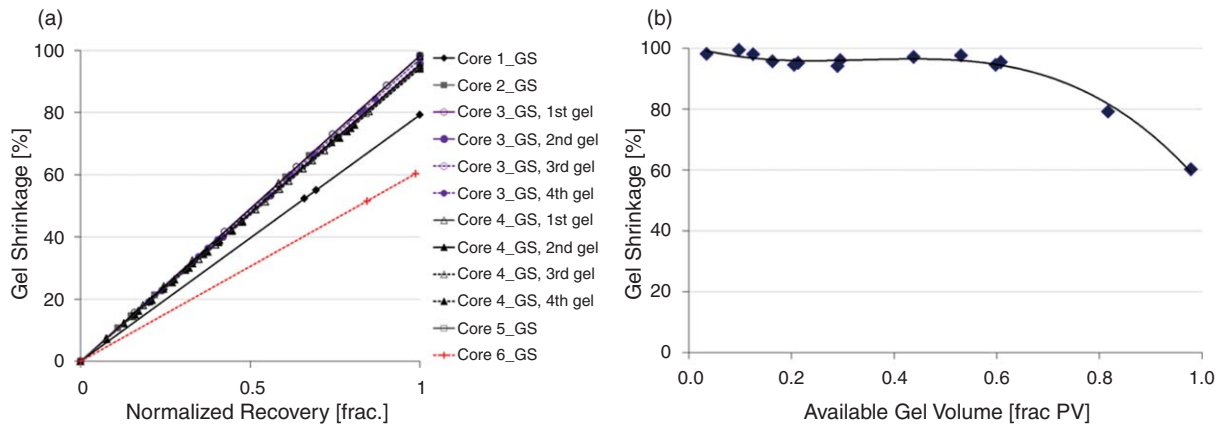


Fig. 12—(a) Gel shrinkage as a function of normalized recovery. (b) Gel shrinkage as a function of available gel volume (PV).

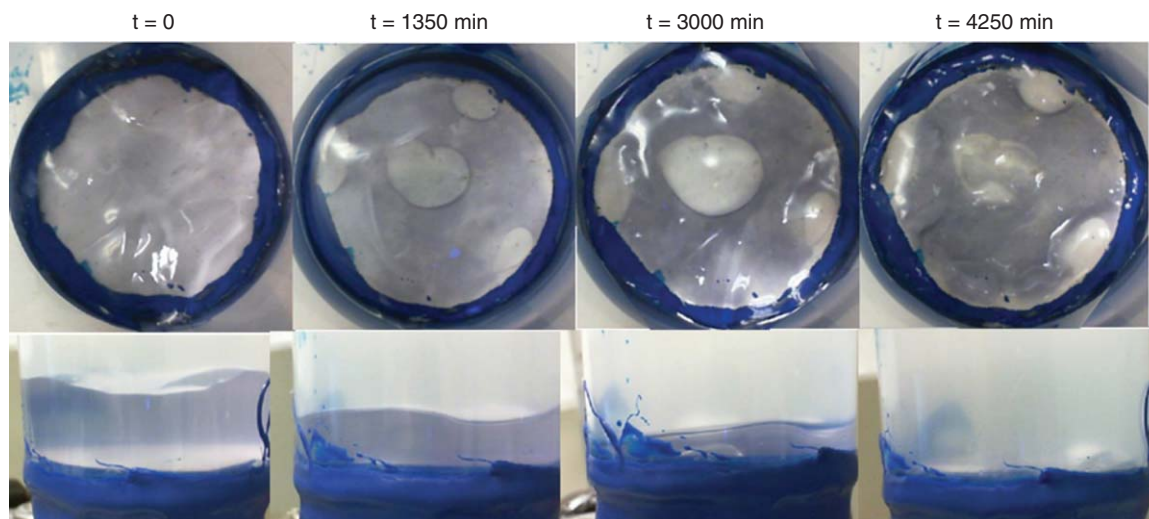


Fig. 13—Core 3_GS, fourth gel placement; shrinkage: 97.16%. Trapped oil drops are observed in the images, with the top row being core seen from a bird's-eye view and the bottom row being the shrinking gel layer seen from the side.

gel will shrink approximately 98% when the available gel volume is less than 0.6 of the matrix PV, which also corresponds to the endpoint for SI for Portland chalk. At approximately 0.6 PV there is a breakpoint where shrinkage is sensitive to the amount of gel available. The breakpoint will probably be dependent on the endpoint for SI, which varies between different rock types but is fairly stable for this core material. In fractured reservoirs, approximately 1% of the PV is typically held in fractures; this implies that the volume of available gel in fractures usually is low compared with the matrix PV, and a fast shrinkage process may be expected because of this.

Fig. 13 shows pictures of the shrinkage process in Core 3_GS, fourth gel placement, at four different timesteps during imbibition. The gel changes color during shrinkage, with a darkening of color meaning that the chrome and polymer concentrations in the gel film are increasing. The degree of shrinkage in this case was 97%, meaning that an initial average gel film thickness of 1.74 cm has shrunk to 0.05 cm because of SI.

The concentration of the polymer-gel layers after imbibition was estimated for AFO cores by use of oil recovery and the weight of the collected gel film. The gel film was successfully collected with consistent results in all five AFO gel experiments. To simplify the calculations, two assumptions were made: (1) that all dehydrated gel was removed from the surface and the weight of the finite gel cake was thus correctly quantified and (2) that no radial gradient of gel layer concentration exists, meaning that the

collected gel had a uniform concentration. Both assumptions are dependent on the immobility of all dehydrated gel (Seright 1999). The results are shown in **Fig. 14a**. The concentration of the collected gel films after SI was estimated to be approximately 4.2 times greater than the original polymer gel concentration for AFO boundary conditions. For gel-shrinkage experiments, the final concentrations were dependent on the available gel volume, and are shown in Fig. 14b. The maximum gel concentration achieved in gel-shrinkage experiments ($C/C_0 \approx 60$) coincides with the maximum concentration reported during extrusion through fractures in earlier work (Seright 2001). This value may represent a maximum achievable gel concentration at moderate pressure conditions and may be associated with the osmotic pressure in the highly concentrated gel, which counteracts further dehydration by capillary forces. For TEO-OW experiments, the gel films were not successfully collected and the gel concentrations therefore were not estimated.

The SI of brine from gel is significant on the core scale at strongly water-wet conditions. On the reservoir scale, the gel-treated area may have less-water-wet conditions or even oil-wet conditions, in which case the capillary forces either will be less dominant or will completely inhibit imbibition of brine from gel. An increased initial gel concentration in the fracture (caused by leakoff, for example) may also slow the imbibition of brine from gel because the gel will be stronger. The effect of gel shrinkage on fracture conductivity was mathematically estimated by use of

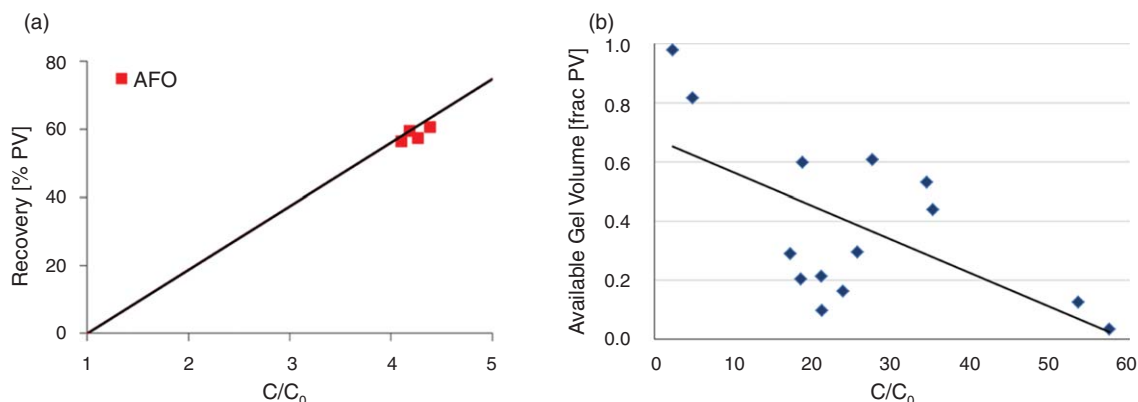


Fig. 14—(a) Concentration of the dehydrated gel layer after AFO imbibition ended was classified by weight measurements and volume recordings. (b) Final concentration divided by original polymer concentration as a function of available gel volume for imbibition during gel-shrinkage experiments.

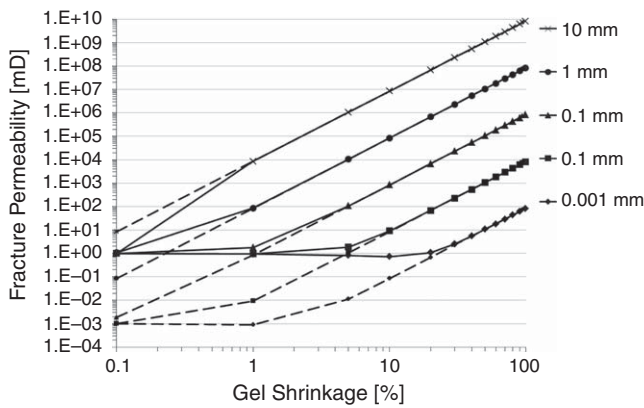


Fig. 15—Fracture permeability as a function of gel shrinkage. The dotted lines reflect an initial polymer concentration of 5%, which may be the case after gel placement with leakoff. The black lines are modeled after an initial polymer concentration of 0.5%, which is also the initial value in all experiments.

the cubic law of Witherspoon et al. (1980), where the absolute permeability of the fracture is a function of fracture aperture (b) only,

$$K_{abs} = b^2/12, \dots \dots \dots (3)$$

and the relationship between gel permeability (K_{gel}) and polymer concentration (C) given by Seright (2006) is

$$K_{gel} = 125 C^{-3}, \dots \dots \dots (4)$$

where K_{gel} is given in μd .

Consider fractures with constant apertures of 0.001 to 10 mm, and filled with gel of initial concentrations of 0.5% (gel of original concentration) and 5% (gel that has experienced leakoff during extrusion), respectively. Gel shrinkage was implemented in the calculations by considering flow through the fracture as darcy flow in parallel layers, where layer one is the gel, of which thickness will decrease and concentration will increase with gel shrinkage, and layer two is the part of the fracture open to flow, and the opening will be directly proportional to the gel shrinkage. The initial permeability of the system equals the gel permeability calculated from Eq. 4. **Fig. 15** shows the resulting system permeability calculated as a function of gel shrinkage when initial gel concentration was 0.5% (solid lines) and 5% (dotted lines). The calculations showed that 1% gel shrinkage will increase the permeability of the widest fracture system (10 mm) by 10,000 md and the permeability of the 1-mm fracture system by 100 md, whereas fractures less than 1 mm will experience a permeability increase of <10 md. After the gel has shrunk 10%, the wide fractures will have permeabilities 10^7 and 10^5 md higher than the initial fracture permeability, respectively, and tighter fractures will have had a permeability increase of up to 1,000 md. The influence of gel shrinkage on fracture-system permeability is highly dependent on the fracture aperture. In wide fractures, severe permeability increase may be seen even at low degrees of gel shrinkage.

Discussion

Imbibition of brine from gel was observed in all core materials and by use of both boundary conditions, AFO and TEO-OW. The results prove that the presence of capillary forces is sufficient to dehydrate aged polymer gel. This indicates that gel behavior during and after placement may be affected by properties that influence capillary forces, such as pore size, wettability, and interfacial tension (IFT). It is therefore important to consider such properties to quantify and predict gel behavior in a reservoir.

SI From Gel. The measured SI rates suggest a difference between a gel/oil system and a conventional water/oil system.

The differences were more pronounced in cores of higher VSR, and included lowering of the initial imbibition rate by a factor of 10 when the cores were submerged in gel. The decrease in recovery rate as a function of VSR was observed throughout all experiments. Changes in imbibition and production rate between water/oil and gel/oil cases are because of polymer-gel characteristics or polymer-gel/core-surface interactions. The crosslinked polymer chains constituting the gel will not enter porous rock with the given pore-throat radii; hence, water alone enter the cores by SI. The in-situ displacement process is thus regular two-phase water/oil flow. However, the imbibition of water from gel dehydrates the gel, building up a more-concentrated gel film at the core surface. Seright (2006) defined a relationship between polymer concentration and gel permeability (Eq. 4), which states that increasing polymer concentration decreases gel permeability. The decrease in gel permeability increases the skin factor on the core surface and induces an additional pressure drop across the concentrated gel layer, between the core surface and the fresh polymer gel. The endpoint for SI, defined by zero capillary pressure on the capillary pressure curve in water/oil systems, may not be reached if the skin factor is high enough to counteract the capillary forces. At high VSR, for example, in experiments by use of TEO-OW boundary conditions, the skin factor will increase quickly. This may partially explain why the endpoint for SI is not reached in some TEO-OW experiments by continued imbibition in gel. The dependency on the bulk volume available for imbibition compared with the open surface indicated that a faster imbibition process and a higher degree of oil recovery and gel shrinkage may be seen in highly fractured reservoirs compared with reservoirs of less fracture intensity.

Gel Shrinkage Caused by SI. In gel treatments of some reservoirs, gel is injected over a relatively short period (for example, approximately 1 day for many production-well treatments) to reduce fracture conductivity. Several authors have reported gel treatments to lose efficiency over time (White et al. 1973; Seright 2003; Portwood 2005). Our work clearly shows that the capillary forces acting in the matrix of oil-saturated porous rock are sufficiently strong to dehydrate gel and cause it to shrink. The shrinkage of gel may open large parts of the gel-treated fractures to flow and decrease the efficiency of the gel treatment over time. The reduced imbibition rates in gel/oil systems compared with brine/oil systems corroborate that the effects of shrinkage by SI may involve a slow process and may require time before they are manifested by reduced blocking efficiency.

In other cases, especially injection wells in naturally fractured reservoirs, gel injection occurs over the course of 1 to 4 weeks (Hild and Wackowski 1999). For these cases, dehydration of the gel by imbibition may occur largely at the same time as dehydration during the gel-extrusion process. Consequently, effects of subsequent gel shrinking may be less important.

Implications of Imbibition on Gel Treatments in Fields. The results presented in this paper all feature cores with large volumes of gel available for imbibition, effectively constituting a large (infinite) fracture volume compared with matrix PV. In naturally fractured reservoirs, the fracture volume is usually less than 3% of the total PV and frequently less than 1% of PV. This implies that a small fraction of SI from the gel-filled fracture to the matrix may shrink the gel enough to reduce its blocking efficiency. The high VSR present in a reservoir also implies that the SI process may continue for a long time, in fact as long as a positive capillary pressure, or a capillary pressure above the osmotic gel pressure, is present in the matrix. The following list defines cases of special concern, where the findings in this study may be crucial to gel-treatment efficiency.

1. Oil-bearing zones. The capillary forces are strongly dependent on saturation; in water-wet systems, areas of high oil saturation are most prone to imbibition. It may thus be expected that the influence of imbibition on gel treatments is most prominent in areas of high continued oil saturation, including oil-production

zones and oil-production wells. This observation may also be exploited in special circumstances; “good fractures” that allow water to be distributed deep into a reservoir may have high oil saturations in the adjacent matrix. So, imbibition that compromises the gel may promote water entry into and oil displacement from these areas during gel placement. In contrast, for areas with fractures that have allowed severe water channeling, high water saturations in the surrounding matrix may cause a lower level of gel dehydration, and therefore the gel may still provide a substantial reduction in fracture conductivity.

2. Gel treatments by use of immature gels (gelant). When injecting gelant, the polymer and crosslinker concentrations will at best remain constant, but may also be diluted by formation water, may experience crosslinker diffusion to the matrix, and so forth. This means that the gel forming in the fracture has a concentration that is equal to or lower than the injected concentration. This study shows that the chance of imbibition occurring at typical gelant compositions is high and the gel treatment is likely to lose efficiency over time, provided that a potential for SI is present. By use of formed gels, a leakoff effect may take place during extrusion through fractures, which increases the concentration of the gel. A higher gel concentration means a more rigid gel in which molecular bonds will be stronger. A critical gel concentration for this particular gel was observed to be $C/C_0 \approx 60$. At this concentration, an osmotic pressure in the gel is suspected to counteract further dehydration. Studies have shown that this concentration may be achieved during extrusion of formed gel through fractures (Seright 2001), and a gel treatment by use of mature gels may thus be less prone to SI. The effect of gelant leakoff to the matrix during placement of immature gels may be of importance and will be part of our future work.

3. Wide fractures. Calculations performed in this work, and illustrated in Fig. 15, showed that gel dehydration will have a more severe effect in wide fractures, and will be a concern for gel treatments by use of both immature and mature gels. The leakoff process during injection of mature gels is less efficient in wider fractures (Seright 2003), and the gel concentration after placement is thus lower. In gels of lower concentration, SI effects are more likely to occur. Note that the calculations are performed on the basis of fractures of a constant aperture. In real reservoirs, fractures may be filled with deposits and not be fully open, which may influence gel dehydration both during injection (higher gel concentration caused by improved leakoff) and after placement (less imbibition and shrinkage because of a higher concentration gel in the fracture, or less impact from shrinkage because of more narrow fractures). Also, recall that fractures that are filled completely with sand or other substances are porous media, and formed gels will not flow (extrude) through porous media (Seright 2001). Consequently, the fracture must be “open” and have some effective average fracture width in order for formed gels to propagate. Previous work (Seright 2001, 2003) has shown that this effective average fracture width is an important factor for determining the pressure gradient for gel extrusion and the degree of gel dehydration.

Adding surfactants to the polymer gel may decrease SI of water by lowering the IFT between brine and oil. Surface-active agents may also aid leakoff water to overcome the capillary threshold pressure imbedded in an oil-wet reservoir and improve dehydration of gel during extrusion through oil-wet fractures. Oil-based gels may also prevent shrinkage in regions where SI of water is an important mechanism. Further laboratory work is planned to investigate the severity of gel dehydration in systems of less-water-wet characteristics, in core material exhibiting lower capillary forces, and by use of gelant in addition to aged polymer gel.

Conclusions

- Capillary forces in outcrop chalk, limestone, and sandstone were strong enough to dehydrate aged polymer gel.
- A significant reduction in gel volume caused by SI was seen.
- The degree and rate of gel shrinkage were dependent on the available volume of gel present close to the core surface.

When a gel volume less than the moveable oil volume was available for imbibition, gel shrinkage of approximately 98% was recorded.

- The fastest gel shrinkage is experienced in the core with the lowest available gel volume for imbibition.
- Gel shrinkage may severely affect the gel blockage efficiency by opening parts of the fracture volume to flow. The influence of gel shrinkage on fracture conductivity is highly dependent on the fracture aperture, and wide fractures may experience severe conductivity increase, even at low degrees of shrinkage.
- Gel shrinkage may be most severe in oil-bearing zones such as oil-production wells; during field treatments by use of gelant; and in wide fractures. One suggestion to avoid large-scale shrinkage is to add surfactant to the polymer gel, thereby lowering the IFT.
- The rate of SI of brine bound in aged polymer gel was quantified for strongly water-wet chalk cores by use of both AFO and TEO-OW boundary conditions.
- The imbibition process was highly dependent on the presence of a dehydrated gel layer on the core surface, which introduces a skin factor during imbibition.
- Measuring the rate of SI by use of AFO boundary conditions could be challenging because the oil that was displaced from the core was trapped within the gel, either on the core surface or in the core vicinity. Care must be taken not to remove any part of the gel layer during weighing because that will accelerate the imbibition process.
- In AFO experiments, even though the rate of imbibition was decelerated when a dehydrated gel layer was present, the endpoint saturation was reached in all experiments.
- In TEO-OW experiments, the rates of recovery were reduced and were dependent on the VSR. This ratio was equal to the core length for this particular setup.
- The endpoint for SI was not reached during horizontal TEO-OW experiments by continuous imbibition in gel, because of the dehydrated gel layer on the end face representing a positive skin factor. When the gel layer was removed, SI continued.
- Future work includes gel dehydration in systems of less-water-wet characteristics, in core material exhibiting lower capillary forces, and by use of immature gel in addition to aged polymer gel.

Nomenclature

A_{surf}	= surface area open to flow
b	= fracture aperture
C	= polymer concentration after gel dehydration
C_0	= polymer concentration in original, “injected” gel
K_{abs}	= absolute permeability of a fracture
K_{gel}	= gel permeability
Δm_{max}	= maximum weight change
$\Delta m(t)$	= weight differential as a function of time
$m_{(c+gf),\text{max}}$	= endpoint core weight, including gel film
$m_{(c+gf)}(t)$	= weight of core including gel film as a function of time
$m_{gf,\text{max}}$	= gel film weight at the end of SI
$m_{gf}(t)$	= gel film weight as a function of time
m_i	= initial core weight
R_f	= recovery factor
S_o	= oil saturation
S_w	= water saturation
t_{brine}	= time it takes to reach given S_w during imbibition in brine
t_d	= dimensionless time
t_{gel}	= time it takes to reach given S_w during imbibition in gel
V_b	= bulk volume

Acknowledgments

Two of the authors are indebted to the Norwegian Research Council for financial support.

References

- Al-Sharji, H.H., Grattoni, C.A., Dawe, R.A., et al. 1999. Pore-Scale Study of the Flow of Oil and Water Through Polymer Gels. Paper SPE 56738 presented at SPE Annual Technical Conference and Exhibition, Houston, Texas, 3–6 October. <http://dx.doi.org/10.2118/56738-MS>.
- Brattekkås, B. 2009. EOR by Polymer Gel Extrusion through Fractures: An Experimental Study of Water Leakoff as Function of Flow Rate, Wettability and Relative Permeability. MSc thesis, University of Bergen, Bergen, Norway (June 2009).
- Ekdale, A. A. and Bromley, R. G. 1993. Trace Fossils and Ichnofabric in the Kjølbj Gaard Marl, Uppermost Cretaceous, Denmark. *Bull. Geol. Soc. Denmark* **31**: 107–119.
- Dawe, R.A. and Zhang, Y. 1994. Mechanistic Study of the Selective Action of Oil and Water Penetrating into a Gel Emplaced in a Porous Medium. *J. Pet. Sci. Eng.* **12** (2): 113–125. [http://dx.doi.org/10.1016/0920-4105\(94\)90011-6](http://dx.doi.org/10.1016/0920-4105(94)90011-6).
- Graue, A., Nesse, K., Baldwin, B.A., et al. 2002. Impact of Fracture Permeability on Oil Recovery in Moderately Water-Wet Fractured Chalk Reservoirs. Paper SPE 75165 presented at SPE/DOE Improved Oil Recovery Symposium, Tulsa, Oklahoma, 13–17 April. <http://dx.doi.org/10.2118/75165-MS>.
- Handy, L.L. 1960. Determination of Effective Capillary Pressures for Porous Media from Imbibition Data. *Pet. Trans. AIME* **219**: 75–80.
- Hild, G.P. and Wackowski, R.K. 1999. Reservoir Polymer Gel Treatments To Improve Miscible CO₂ Flood. *SPE Res Eval & Eng* **2** (2): 196–204. <http://dx.doi.org/10.2118/56008-PA>.
- Hjuler, M.L. 2007. Diagenesis of Upper Cretaceous Onshore and Offshore Chalk from the North Sea Area. PhD dissertation, Technical University of Denmark, Kongens Lyngby, Denmark (August 2007).
- Klein, E. and Reuschlè, T. 2003. A Model for the Mechanical Behaviour of Bentheim Sandstone in the Brittle Regime. *Pure Appl. Geophys.* **160** (5–6): 833–849. <http://dx.doi.org/10.1007/PL00012568>.
- Krishnan, P., Asghari, K., Willhite, G.P., et al. 2000. Dehydration and Permeability of Gels Used in In-Situ Permeability Modification Treatments. Paper SPE 59347 presented at SPE/DOE Improved Oil Recovery Symposium, Tulsa, Oklahoma, 3–5 April. <http://dx.doi.org/10.2118/59347-MS>.
- Liu, J. and Seright, R.S. 2001. Rheology of Gels Used for Conformance Control in Fractures. *SPE J.* **6** (2): 120–125. <http://dx.doi.org/10.2118/70810-PA>.
- Ma, S., Morrow, N.R. and Zhang, X. 1997. Generalized Scaling of Spontaneous Imbibition Data for Strongly Water-Wet Systems. *J. Pet. Sci. Eng.* **18** (3–4): 165–178. [http://dx.doi.org/10.1016/S0920-4105\(97\)00020-X](http://dx.doi.org/10.1016/S0920-4105(97)00020-X).
- Mason, G., Fischer, H., Morrow, N.R., et al. 2009. Effect of Sample Shape on Counter-Current Spontaneous Imbibition Production vs. Time Curves. *J. Pet. Sci. Eng.* **66** (3–4): 83–97. <http://dx.doi.org/10.1016/j.petrol.2008.12.035>.
- Portwood, J.T. 1999. Lessons Learned from Over 300 Producing Well Water Shut-off Gel Treatments. Paper SPE 52127 presented at SPE Mid-Continent Operations Symposium, Oklahoma City, Oklahoma, 28–31 March. <http://dx.doi.org/10.2118/52127-MS>.
- Portwood, J.T. 2005. The Kansas Arbuckle Formation: Performance Evaluation and Lessons Learned From More Than 200 Polymer-Gel Water-Shutoff Treatments. Paper SPE 94096 presented at SPE Productions and Operations Symposium, Oklahoma City, Oklahoma, 17–19 April. <http://dx.doi.org/10.2118/94096-MS>.
- Riskedal, H. 2008. Wettability and Rock Characterization of Heterogeneous Limestone Utilizing NMR. MSc thesis, University of Bergen, Bergen, Norway (April 2008).
- Romero-Zeron, L., Manalo, F. and Kantzas, A. 2003. Characterization of Crosslinked Gel Kinetics and Gel Strength Using NMR. Paper SPE 86548 presented at SPE International Symposium and Exhibition on Formation Damage Control, Lafayette, Louisiana, 18–20 February. <http://dx.doi.org/10.2118/86548-MS>.
- Rousseau, D., Chauveteau, G., Renard, M., et al. 2005. Rheology and Transport in Porous media of New Water Shutoff/Conformance Control Microgels. Paper SPE 93254 presented at SPE International Symposium on Oilfield Chemistry, The Woodlands, Texas, 2–4 February. <http://dx.doi.org/10.2118/93254-MS>.
- Schutjens, P.M.T.M., Hausenblas, M., Dijkshoorn, M., et al. 1995. The Influence of Intergranular Microcracks on the Petrophysical Properties of Sandstone—Experiments to Quantify Effects of Core Damage. Oral presentation given at the International Symposium of the Society of Core Analysts, San Francisco, California, 12–14 September.
- Seright, R.S. 2003. An Alternative View of Filter-cake Formation in Fractures Inspired by Cr (III)-Acetate-HPAM Gel Extrusion. *SPE Prod & Fac* **18** (1): 65–72. <http://dx.doi.org/10.2118/81829-PA>.
- Seright, R.S. 2001. Gel Propagation Through Fractures. *SPE Prod & Fac* **16** (4): 225–231. <http://dx.doi.org/10.2118/74602-PA>.
- Seright, R.S. 2006. Optimizing Disproportionate Permeability Reduction. Paper SPE 99443 presented at SPE/DOE Improved Oil Recovery Symposium, Tulsa, Oklahoma, 22–26 April. <http://dx.doi.org/10.2118/99443-MS>.
- Seright, R.S. 1999. Polymer Gel Dehydration During Extrusion Through Fractures. *SPE Prod & Fac* **14** (2): 110–116. <http://dx.doi.org/10.2118/56126-PA>.
- Seright, R.S., Lane, R.H. and Sydansk, R.D. 2003. A Strategy for Attacking Excess Water Production. *SPE Prod & Fac* **18** (3): 158–169. <http://dx.doi.org/10.2118/84966-PA>.
- Sydansk, R.D. 1993. Acrylamide-Polymer/Chromium (III)-Carboxylate Gels for Near Wellbore Matrix Treatments. *SPE Advanced Technology Series* **1** (1): 146–152. <http://dx.doi.org/10.2118/20214-PA>.
- Sydansk, R.D. and Southwell, G.P. 2000. More Than 12 Years of Experience with a Successful Conformance-Control Polymer Gel Technology. Paper SPE 62561 presented at SPE/AAPG Western Regional Meeting, Long Beach, California, 19–23 June. <http://dx.doi.org/10.2118/62561-MS>.
- Tipura, L. 2008. Wettability Characterization by NMR T₂ Measurements in Edwards Limestone. MSc thesis, University of Bergen, Borgen, Norway (June 2008).
- Vikund, B.G., Morrow, N.R., Ma, S., et al. 1998. Initial Water Saturation and Oil Recovery from Chalk and Sandstone by Spontaneous Imbibition. Oral presentation given at the International Symposium of Society of Core Analysts, The Hague, The Netherlands, 14–16 September.
- Vossoughi, S. 2000. Profile Modification Using In Situ Gelation Technology—A Review. *J. Pet. Sci. Eng.* **26** (1–4): 199–209. [http://dx.doi.org/10.1016/S0920-4105\(00\)00034-6](http://dx.doi.org/10.1016/S0920-4105(00)00034-6).
- White, J.L., Goddard, J.E. and Phillips, H.M. 1973. Use of Polymers to Control Water Production in Oil Wells. *J. Pet. Tech.* **25** (2): 143–150. <http://dx.doi.org/10.2118/3672-PA>.
- Willhite, G.P. and Pancake, R.E. 2004. Controlling Water Production Using Gelled Polymer Systems. Paper SPE 89464 presented at SPE/DOE Improved Oil Recovery Symposium, Tulsa, Oklahoma, 17–21 April. <http://dx.doi.org/10.2118/89464-MS>.
- Witherspoon, P.A., Wang, J.S.W., Iwai, K., et al. 1980. Validity of Cubic Law for Fluid Flow in a Deformable Rock Fracture. *Water Resour. Res.* **16** (6): 1016–1024. <http://dx.doi.org/10.1029/WR016i006p1016>.
- Zhang, H. and Bai, B. 2011. Preformed-Particle-Gel Transport through Open Fractures and Its Effect on Water Flow. *SPE J.* **16** (2): 388–400. <http://dx.doi.org/10.2118/129908-PA>.

Bergit Brattekkås holds an MS degree in reservoir physics from the University of Bergen, Norway, and is currently a PhD candidate at the Department of Physics and Technology at the University of Bergen. Her main research interests are multiphase-fluid flow in porous media and enhanced-oil-recovery (EOR) techniques for heterogeneous reservoirs, including polymer gels, foam, and CO₂ injection.

Åsmund Haugen holds MS and PhD degrees in reservoir physics from the University of Bergen. His research interests are flow parameters, fluid flow in heterogeneous reservoirs, emphasizing fracture/matrix interaction; wettability effects; fluid visualization; and EOR techniques including foam, polymer gel, and CO₂ injection. Haugen is currently senior engineer within Special Core Analysis in Statoil ASA.

Arne Graue is professor of physics at the Department of Physics and Technology, University of Bergen, where he is head of the Petroleum and Process Technology Research Group. His scientific interest is within reservoir physics, emphasizing heterogeneous and fractured reservoirs, multiphase flow in porous media, in-situ fluid-saturation imaging, laboratory investigation of integrated EOR techniques, CO₂ sequestration, and gas

hydrates. Graue has published more than 200 scientific publications and supervised 114 PhD and MS students. He holds an MS degree in experimental nuclear physics and a PhD degree in reservoir physics, both from the University of Bergen. Graue has been an invited visiting scientist/professor at the Massachusetts Institute of Technology, Cambridge, Massachusetts; the University of Wyoming, Laramie, Wyoming; the University of Kansas, Lawrence, Kansas; and at ConocoPhillips Research Center. He is currently the international coordinator for a collaboration of 11 universities in five countries on EOR in fractured reservoirs; coordinator for carbon-capture-and-storage research collaboration between Norway and the USA; petroleum and carbon-capture-utilization-and-storage adviser to

Norway's consul general in Houston; Chairman of the Executive Board of the Petroleum Research School of Norway, where all universities in Norway are represented, and Chairman of the Board of NorTex Petroleum Cluster.

Randy Seright is a senior engineer at the Petroleum Recovery Research Center of New Mexico Tech in Socorro, New Mexico, where he has worked for the past 26 years. He holds a PhD degree in chemical engineering from the University of Wisconsin, Madison. Seright has been a registered professional engineer since 1983. He received the SPE/US Department of Energy IOR Pioneer award in 2008 for his work on the use of polymer and gels to improve oil recovery.